

# GALAXIES AT REDSHIFTS $z > 5$

Kenneth M. Lanzetta<sup>1</sup>, H.-W. Chen<sup>1</sup>, S. Pascarelle<sup>1</sup>, N. Yahata<sup>1</sup>

<sup>1</sup> *State University of New York at Stony Brook, Stony Brook, U.S.A.*

## Abstract

Here we describe our attempts to establish statistically complete samples of very high redshift galaxies by obtaining photometric redshifts of galaxies in Medium Deep Survey (MDS) fields and photometric and spectroscopic redshifts of galaxies in very deep STIS slitless spectroscopy fields. On the basis of this analysis, we have identified galaxies of redshift  $z = 4.92$  in an MDS field and of redshift  $z = 6.68$  in a very deep STIS field.

## 1 Introduction

Our photometric redshift technique applied to observations of the Hubble Deep Field (HDF) has identified galaxies at redshifts up to and beyond  $z = 6$  ([1], [2]). The recent confirmation of two of these measurements at redshifts  $z > 5$  ([3], [4]) has established that broad-band redshift measurement techniques can accurately and reliably identify high-redshift galaxies—not only in a general sense, distinguishing high- from low-redshift galaxies, but also in a specific sense, establishing redshifts to within relative errors of typically  $\Delta z/(1+z) < 15\%$ .

Building on the success of the broad-band redshift measurement techniques, we have sought to establish statistically complete samples of very high redshift galaxies by means of four distinct methods applied to four distinct collections of observations: (1) photometric redshifts of galaxies in the HDF, (2) photometric redshifts of galaxies in Medium Deep Survey (MDS) fields, (3) photometric and spectroscopic redshifts of galaxies in very deep STIS slitless spectroscopy fields, and (4) photometric redshifts of infrared detected (and optical non-detected) galaxies in the HDF. In principle, the optical-wavelength observations are sensitive to galaxies at redshifts as large as  $z \approx 7$ , while the infrared-wavelength observations are sensitive to galaxies at redshifts as large as  $z \approx 17$ .

Here we describe initial results of the second and third of these programs, namely of photometric redshifts of galaxies in MDS fields and photometric and spectroscopic redshifts of galaxies in very deep STIS slitless spectroscopy fields.

## 2 Photometric redshifts of galaxies in MDS fields

First, we have sought to measure photometric redshifts of galaxies in MDS fields. The MDS ([5]) currently spans more than 450 fields, which have been observed using HST with WFPC2 and the F814W, F606W, and (in some cases) the F450W filters. These observations are, of course, not as deep as the observations of the HDF. But what these observations lack in

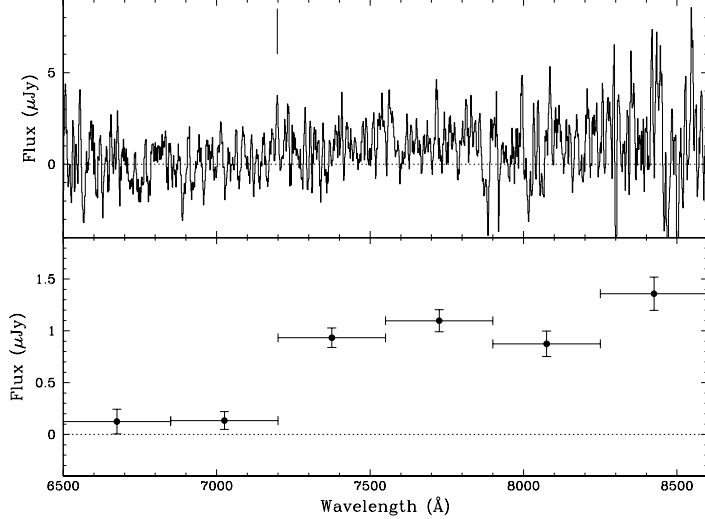


Figure 1: Spectrum obtained with the KPNO 4 m telescope of a high-redshift galaxy identified in an MDS field. Upper panel shows spectrum (of pixel size 5 Å boxcar smoothed by three pixels), and lower panel shows spectrum cast into 350 Å bins. Tick mark in upper panel indicates a statistically significant emission line. We interpret the emission line at  $\lambda = 7200$  Å as Ly $\alpha$  and the continuum break at  $\lambda = 7200$  Å as the Ly $\alpha$  decrement, in which case the redshift of the galaxy is  $z = 4.92$ .

depth, they make up for in breadth, covering an angular area of  $\approx 0.6$  deg $^2$  to a  $5\sigma$  point source limiting magnitude threshold of typically  $AB(8140) \approx 27.0$ . Our previous application of the photometric redshift technique to the HDF ([1], [2]) incorporated observations spanning seven photometric bands. In contrast, our application of the photometric redshift technique to the MDS fields incorporates observations spanning only two or three photometric bands, which of course makes photometric redshift measurement more difficult. But given sufficiently small photometric errors, continuum break features indicative of high-redshift galaxies (i.e. the Lyman limit and the Ly $\alpha$  decrement) can be *unambiguously* distinguished from continuum break features indicative of low-redshift galaxies (i.e. the 4000 Å break) because the amplitude of the largest continuum breaks observed in low-redshift galaxies or main-sequence stars is  $\approx 3$  (see [4] and references therein), whereas the amplitude of the Lyman continuum break is in principle infinite or close to it. The key, then, is to apply the two- or three-band photometric redshift technique only in cases where the photometric errors are small enough to distinguish the Lyman break from other continuum features to a high level of significance—i.e. to bright (through the F814W filter) galaxies or to deep images. We have so far applied this analysis to a portion of the MDS observations in order to identify candidate galaxies for confirming spectroscopy.

Figure 1 shows a spectrum obtained with the KPNO 4 m telescope of a high-redshift galaxy identified in an MDS field. The spectrum is characterized by an emission line at  $\lambda = 7200$  Å, which we interpret as Ly $\alpha$ , and by a continuum break at  $\lambda = 7200$  Å, which we interpret as the Ly $\alpha$  decrement, in which case the redshift of the galaxy is  $z = 4.92$ . Based on an initial analysis, we expect that  $\approx 65$  galaxies of redshift  $z > 5$  be identified in the MDS fields.

### 3 Photometric and spectroscopic redshifts of galaxies in very deep STIS slitless spectroscopy observations

Second, we have sought to measure photometric and spectroscopic redshifts of galaxies in very deep STIS slitless spectroscopy fields. At near-infrared wavelengths, where background sky light is the dominant source of noise, the Hubble Space Telescope (HST) using the Space Telescope Imaging Spectrograph (STIS) is more sensitive than the Keck telescope because from space (1) the sky is fainter and (2) the spatial resolution is higher. To exploit the unique sensitivity of STIS at near-infrared wavelengths, the Space Telescope Science Institute and the STIS instrument team at the Goddard Space Flight Center initiated the STIS Parallel Survey, in which deep STIS observations are obtained in parallel with other observations [6]. From among the observations so far obtained by the Survey, we selected for analysis very deep observations acquired in slitless spectroscopy mode, because these observations are best suited for identifying distant galaxies.

The difficulty of slitless spectroscopy is that the objects can overlap along the dispersion direction. We have overcome this difficulty by developing and applying a new method of analyzing slitless spectroscopy observations that makes optimal use of the direct and dispersed images that are recorded as part of a normal sequence of observation. Specifically, we use the direct image to determine not only the exact locations but also the exact two-dimensional spatial profiles of the spectra on the dispersed image. These spatial profiles are crucial because they provide the “weights” needed to optimally extract the spectra and the models needed to deblend the overlapping spectra and determine the background sky level. Our analysis proceeds in three steps: First, we identify objects in the direct image, using standard source extraction programs. Next, we model each pixel of the dispersed image as a linear sum of contributions from relevant portions of all overlapping neighboring objects and background sky. Finally, we minimize  $\chi^2$  between the model and the data with respect to the model parameters to form optimal one-dimensional spectra.

We measure redshifts from the optimal one-dimensional spectra by means of *both* broad-band continuum features and narrow-band emission and absorption features. Specifically, we measure photometric redshifts using a variation of the photometric redshift technique described previously by [1], and we seek to verify the photometric redshifts by identifying confirming narrow emission and absorption features. At low redshifts, the most prominent broad-band feature is the 4000 Å break and the most prominent narrow-band features are the [O II] emission line and the Ca II H and K absorption lines, while at high redshifts, the most prominent broad-band feature is the Ly $\alpha$  decrement and the most prominent narrow-band feature is the Ly $\alpha$  emission line.

Figure 2 shows examples of photometric and spectroscopic redshifts of galaxies in very deep STIS slitless spectroscopy fields. The spectrum of the highest-redshift galaxy is characterized by an emission line at  $\lambda = 7200$  Å, which we interpret as Ly $\alpha$ , and by a continuum break at  $\lambda = 7200$  Å, which we interpret as the Ly $\alpha$  decrement, in which case the redshift of the galaxy is  $z = 6.68$ . Based on an initial analysis, we expect that redshifts of a large fraction of galaxies in the STIS field will be identified.

**Acknowledgements.** This research was supported by NASA grant NAGW-4422 and NSF grant AST-9624216.

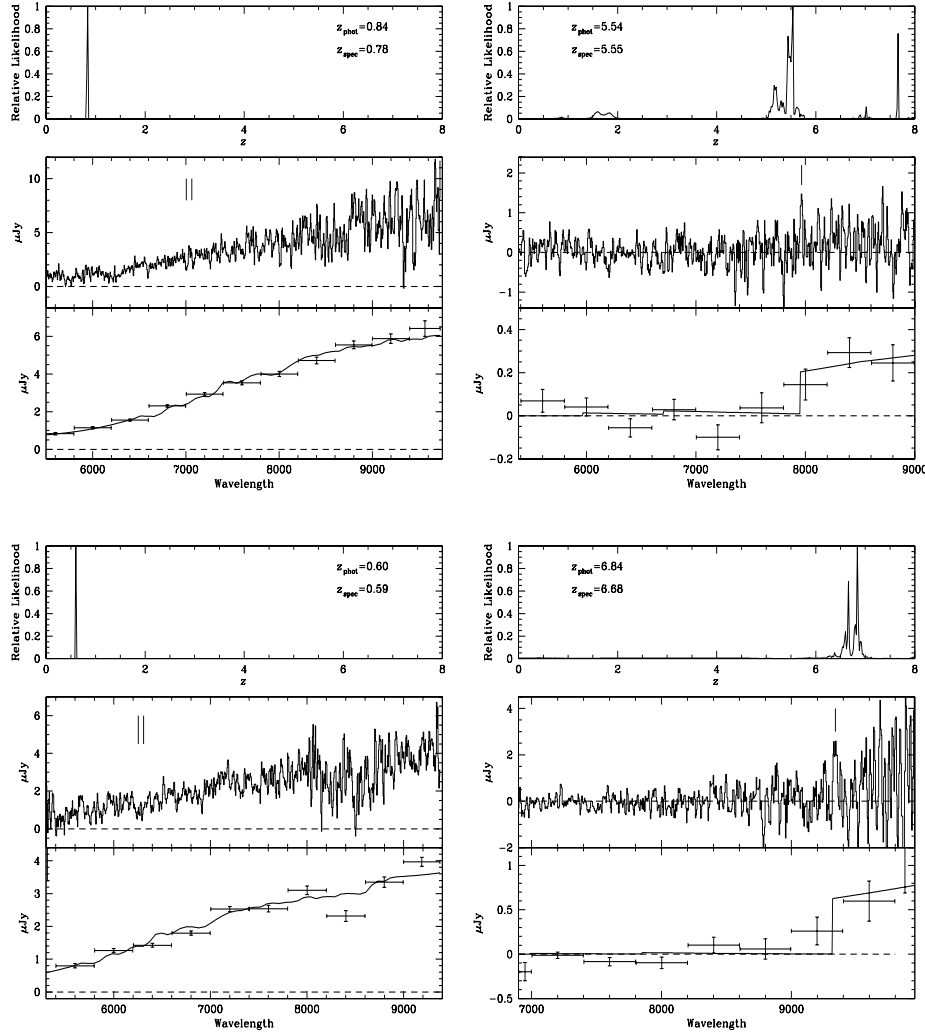


Figure 2: Examples of photometric and spectroscopic redshifts of galaxies in very deep STIS slitless spectroscopy fields. For each example, top panel shows redshift likelihood function, middle panel shows spectrum (of pixel size 5  $\text{\AA}$  boxcar smoothed by three pixels), and bottom panel shows spectrum cast into 400  $\text{\AA}$  bins together with best-fit spectrophotometric template spectrum. Tick marks indicate statistically significant emission or absorption lines.

## References

- [1] Lanzetta, K. M., Yahil, A., & Fernández-Soto, A. 1996, *Nature* **381**, 759
- [2] Fernández-Soto, A., Lanzetta, K. M., & Yahil, A. 1998, *Astrophys. J.* **in press**,
- [3] Weymann, R. J., Stern, D., Bunker, A., Spinrad, H., Chaffee, F. H., Thompson, R. I., & Storrie-Lombardi, L. J. 1998, *Astrophys. J.* **in press**,
- [4] Spinrad, H. Stern, D., Bunker, A., Dey, A., Lanzetta, K., Yahil, A., Pascarelle, S., & Fernández-Soto, A. 1998, *Astron. J.* **in press**,
- [5] Ratnatunga K. U., Griffiths, R. E., & Ostrander, E. J. 1998, in preparation
- [6] Gardner, J. et al. 1998, *Astrophys. J.* **492**, L99